Modern Pathology (2020) 33:1945–1960
https://doi.org/10.1038/s41379-020-0554-8

ARTICLE

Mucinous carcinoma with micropapillary features is morphologically, clinically and genetically distinct from pure mucinous carcinoma of breast

Peng Sun[1,2] · Zaixuan Zhong[3] · Qianyi Lu[1,4] · Mei Li[1,2] · Xue Chao[1,2] · Dan Chen[3] · Wenyan Hu[3] · Rongzhen Luo[1,2] · Jiehua He[1,2]

Received: 27 February 2020 / Revised: 5 April 2020 / Accepted: 5 April 2020 / Published online: 1 May 2020

Abstract

Micropapillary features are seen in pure mucinous carcinoma of breast (PMC), which is termed mucinous carcinoma with micropapillary features (MPMC). However, whether MPMC can be identified as a morphologically, clinically or genetically distinct entity from PMC remains controversial. In this study, a retrospective review of 161 cases of breast mucinous carcinoma was conducted to assess the clinicopathologic features, prognostic implications, and genomic alterations of MPMC and PMC. MPMCs were identified in 32% of mucinous carcinomas showing an excellent interobserver agreement (ICC = 0.922). MPMCs occurred at a younger age and exhibited higher nuclear grade, more frequent lymph nodal metastasis, lymphovascular invasion, and HER2 amplification compared with PMCs. Survival analyses revealed that MPMCs show decreased progression-free survival compared with PMCs in both unmatched and matched cohorts. A similar outcome of distant disease-free survival was observed only in the unmatched cohort. However, no statistical difference in recurrence score was observed between MPMC and PMC using a 21-gene assay. Notably, both MPMCs and PMCs displayed low mutation burden, common mutations affecting TTN, GATA3, SF3B1, TP53, recurrent 6q14.1-q27 losses, and 8p11.21-q24.3 gains. GATA3, TP53, and SF3B1 were recurrently mutated in MPMCs, while PIK3CA mutations were exclusively detected in PMCs. Moreover, MPMCs harbored 17q and 20q gains as well as 17p losses, while PMCs displayed gains at 6p. PI3K-Akt, mTOR, ErbB, and focal adhesion pathways were more frequently deregulated in MPMCs than in PMCs, which may responsible for the aggressive tumor behavior of MPMCs. Our findings suggest that MPMC is morphologically, clinically, and genetically distinct from PMC.

Introduction

Mucinous carcinoma is a rare and special subtype of breast carcinoma that usually occurs in postmenopausal and elderly women [1–3]. It accounts for 1–7% of all the breast carcinoma and is associated with good prognosis [3–5]. Pure mucinous carcinoma (PMC) possesses >90% of mucinous component and displays a more favorable clinical outcome than mixed mucinous carcinoma which has ~50–90% of mucinous component [3, 6–8]. Several

These authors contributed equally: Peng Sun, Zaixuan Zhong, Qianyi Lu

Supplementary information The online version of this article (https://doi.org/10.1038/s41379-020-0554-8) contains supplementary material, which is available to authorized users.

✉ Peng Sun
sunpeng1@sysucc.org.cn

✉ Jiehua He
hejh@sysucc.org.cn

[1] State Key Laboratory of Oncology in South China; Collaborative Innovation Center for Cancer Medicine, Guangzhou 510060, P.R. China

[2] Department of Pathology, Sun Yat-sen University Cancer Center, Guangzhou 510060, P.R. China

[3] Top Gene Tech (Guangzhou) Co., Ltd, Guangzhou 510623, P.R. China

[4] Department of Medical Oncology, Sun Yat-sen University Cancer Center, Guangzhou 510060, P.R. China

previous studies have suggested that PMCs may have foci with a micropapillary pattern consisting of morula-like clusters suspended in tight mucin pools, reminiscent of invasive micropapillary carcinoma, which is named as mucinous carcinoma with micropapillary features (MPMC). Compared with PMC, MPMC tends to occur at a younger age and has a more aggressive tumor behavior, such as more frequent lymph node metastasis (LNM) and lymphovascular invasion (LVI) [8–14]. A retrospective cohort study by Liu et al. [10] showed that PMCs with a >50% micropapillary component had significantly worse prognosis and MPMCs may be identified as a subset of mucin-producing breast carcinomas with biologic behavior between PMC and IMPC. However, other researchers have reported that MPMCs have similar clinicopathological parameters with PMCs, such as low to moderate nuclear grade, low mitotic rate, ER, PR, and rare HER2 amplification [11–13, 15], and that the existing micropapillary component in mucinous carcinoma may not be significantly related to the prognosis of this tumor [11, 14].

Whether MPMC can be identified as a morphologically, clinically or genetically distinct entity is still controversial. Inconsistent outcomes may due to that the criteria for diagnosing MPMC are not clear. For instance, some researchers have suggested that MPMCs should have moderate to high nuclear grade [12, 16, 17] while other cohorts included cases with mild nuclear grade predominantly [10, 11, 14]. Moreover, despite the "inside-out" or "reversed" pattern of EMA or MUC1 expression by immunostaining is referred to as a diagnostic or confirmatory criterion for micropapillae in mucinous carcinoma, Troxell et al. [18] demonstrated that PMCs may exhibit the same EMA/MUC1 "inside-out" pattern. Few studies have focused on the interobserver reliability in the diagnosis of MPMC and the optimal cut-off value for the percentage of micropapillae in mucinous carcinoma (MP%) assessing disease progression and lymph node metastasis. Most importantly, whether MPMCs exhibit distinct genetic features other than PMC, and whether these specific genomic alterations are responsible for the aggressive tumor behavior of MPMCs has yet to be characterized.

To address these issues, we retrospectively reviewed cases diagnosed as mucinous carcinoma of breast at our cancer center. Clinicopathologic features, such as age, tumor size, nuclear grade, histological grade, LVI, LNM, MP% and ER, PR, HER-2, Ki67 status were evaluated. Intraclass correlation coefficient (ICC) was implemented to estimate the agreement among four pathologists for MP%. We also calculated the optimal cut-off value of MP% for disease progression and LNM. The relationships between the clinicopathologic features, LNM, progression-free survival (PFS), and distant disease-free survival (DDFS) were analyzed in both unmatched and matched cohorts using propensity score matching (PSM). We subsequently applied a 21-gene Recurrence Score Assay in selected cases that were pT1-2N0M0, HR+, HER2−. Formalin-fixed paraffin-embedded (FFPE) samples of tumors and adjacent normal tissues from the selected PMCs ($n = 11$) and MPMCs ($n = 10$) were subjected to whole-exome sequencing analysis (WES). The present study aimed to describe the mutational profiles and genomic alterations between MPMCs and PMCs to provide a resource for investigating the contribution of genes and pathways related to aggressive models of MPMCs.

Materials and methods

Cases selection

A flow chart of the cases-selection is shown in Fig. 1. In brief, clinicopathologic data of patients diagnosed as mucinous carcinoma of breast at the Sun Yat-sen University Cancer Center (SYSUCC) during the year 2005–2015 were

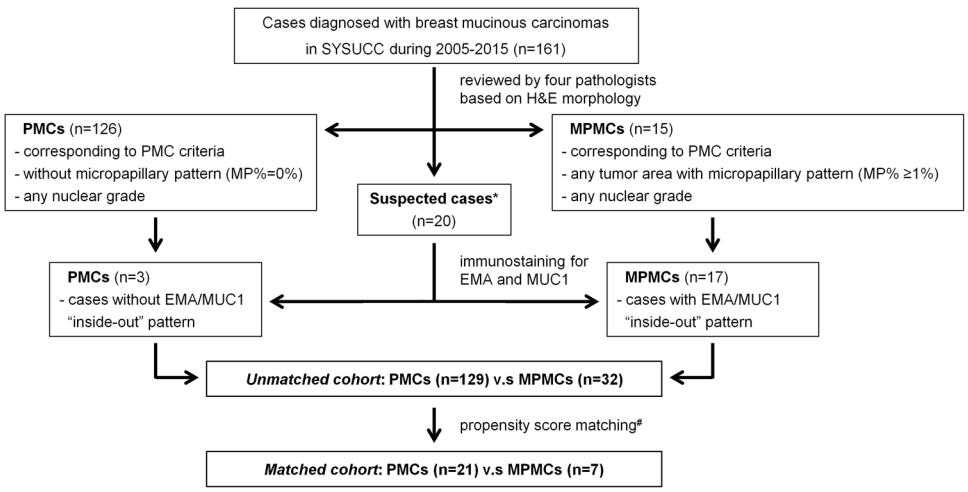

Fig. 1 Flow chart of cases selection. An asterisk inidicates cases with discordant diagnoses were reviewed by four pathologists using slides immunostained with EMA and MUC1 for consensus. #Propensity score matching (PSM) was performed using 3:1 nearest neighbor matching with a caliper of 0.10 to accept a matched pair.

retrieved. All patients were operated at SYSUCC and did not receive neoadjuvant therapy. FFPE tissue specimens, including the tumor, sentinel lymph nodes, and axillary lymph nodes, were stained routinely with hematoxylin and eosin (H&E). The archived H&E slides were retrospectively reviewed by four pathologists (JHH, PS, ML, RZL) to reconfirm the diagnosis of PMC and MPMC. PMC was defined as a tumor composed of >90% of mucinous carcinoma areas with small and uniform cells floating in the extracellular mucin and no micropapillary pattern, based on 2019 WHO classification of breast tumors (5th edition) [19]. Furthermore, type A mucinous carcinomas are relative hypocellular, with a large amount of extracellular mucin, while type B is hypercellular, with various neuroendocrine differentiation. Carcinomas with signet ring-cell differentiation were excluded. Besides, high-grade tumors with sheet, nonmicropapillary tumor cells, and relatively less conspicuous amount of extracellular mucin were considered as invasive breast carcinomas of no special type with mucin production [19], which were also excluded in our study. The histologic criteria for MPMC in the present study were as follow: (1) morphologically corresponding to PMC; (2) any tumor area (MP% ≥ 1%) with micropapillary pattern consisting of morula-like clusters suspended in tight mucin pools, reminiscent of invasive micropapillary carcinoma; (3) demonstrating reversed or stromal-facing EMA and MUC1 on immunostaining. The morphological subclassification and MP% were assessed independently by four pathologists (PS, JHH, RZL, and ML). Suspected cases with discordant diagnoses were reviewed again by all the four pathologists referring to the slides immunostained with EMA and MUC1 until a consensus was reached. MP% was recorded as continuous variable from 0 to 100%.

This study was conducted in accordance with the ethical standards of the research committee of SYSUCC. Formal written informed consent was obtained from all individual participants included in the study.

Clinicopathologic features analysis

Clinicopathological data, including age at diagnosis, laterality, tumor size, nuclear grade, histological grade, LVI, LNM, MP%, local and systemic treatment, tumor recurrence status, distant metastasis, survival, were analyzed. The tumor staging was based on the TNM stage was assessed according to the criteria established by the 8th edition American Joint Committee on Cancer (AJCC 8th) staging manual. ER, PR, and HER2 status were determined on immunohistochemical (IHC) staining. ER and PR status were classified as negative using a cut-off of 1% according to the American Society of Clinical Oncology/College of American Pathologists guidelines [20]. HER2 status was defined as negative with 0, 1+ as well as 2+ on IHC without HER2 gene amplification on fluorescence in situ hybridization (FISH) [21]. HER2 immunoreactivity may yield weak to moderate staining in a U-shaped basolateral pattern in MPMC, which was regarded as equivocal expression (IHC 2+) and reflexed to FISH testing. The percentage of Ki-67 staining cells was assessed in tumor areas on average and recorded as continuous variables. Representative tumor sections were also immunostained with EMA (clone E29, DAKO, Denmark) and MUC1 (clone EPR1023, Abcam, UK).

21-gene expression assay

Eligible FFPE tumor tissues were obtained from MPMCs ($n = 15$) and PMCs ($n = 12$) with axillary node-negative that was hormone receptor-positive (ER+ and/or PR+) and HER2- with tumors of 1.1–5.0 cm in the greatest dimension (T1-2) were selected. A reverse-transcriptase–polymerase-chain-reaction 21-gene assay (Oncotype DX Recurrence Score, Genomic Health) was performed on RNA extracted from the FFPE tissues [22]. All patients had a recurrence score ranging from 0 to 100, with higher scores indicating a greater risk of recurrence. The recurrence score ranges used in this study were defined as low (≤10), intermediate (11–25), and high (≥26). Besides, according to the results from TAILORx trial [22], patients at the age of 50 years or younger who had a recurrence score of 0–15 and those over 50 years of age who had a recurrence score ≤25 were classified as no benefit group, otherwise were classified as benefit group.

Whole-exome sequencing

Eligible FFPE tumor and adjacent normal tissues were obtained from MPMCs with a MP% of ≥50% ($n = 10$) and PMCs with no micropapillary pattern ($n = 11$). Detailed clinicopathological data of the selected 21 patients are provided in Supplementary Table 2. Genomic DNA was extracted from the FFPE slides using the GeneRead DNA FFPE Kit (QIAGEN, German) according to the manufacturer's instructions. Quantification of extracted DNA was performed using the Qubit 3.0. To construct the whole-exome capture library, 500 ng of DNA was randomly sheared into 180–280 bp by Covaris S220 system (Covaris, USA). Fragmented DNA was purified and ligated using the Kapa Hyper Prep kit. Then exons of genes were captured with the AIExome Enrichment Kit V1 (iGeneTech, Beijing, China). Sequencing was performed on MGI2000 (BGI, China) with 100 bp paired-end reads. The Genome Analysis Toolkit (v4.1.2.0) [23] was used to generate analysis-ready bam files from QC-passed Fastq files. Briefly, the sequence data were aligned to human reference genome (hg19) using BWA (v0.7.15) [24]. Picard (v2.20.1) was used to generate sorted

bam files and to mark PCR duplicates. Then, we performed recalibration of base quality score and local realignment of the aligned reads for subsequent accurate variant calling.

Somatic mutation detection

Somatic SNV and indels were detected with Mutect2 following GATK best practices (https://software.broadinstitute.org/gatk/best-practices/). Germline variants were detected using the HaplotypeCaller in GATK with the default parameter. Briefly, a Panel of Normal (PoN) was generated from adjacent normal breast tissues to improve the results of the variant calling analysis. The tumor samples were compared with the matched normal samples to exclude germline variants. To process the Mutect2 output, FilterMutectCalls were applied through several hard filters to detect alignment artifacts, orientation bias artifacts, germline variants, and contamination. Unreliable somatic calls were filtered out if they were found in: (1) PoN, (2) dbSNP [25] and 1000 Genomes datatbase [26]. Mutations were manually inspected using the IGViewer and annotated with ANNOVAR [27]. Tumor mutation burden was defined as the number of somatic mutations per megabase (Mb).

Estimation of copy number

Copy number variants (CNV) were estimated from the WES data using CallCopyRatioSegments according to the GATK best practice with default parameters. First, we collected proportional coverage using target intervals and read data. Then, we created the CNV PoN based on proportional coverage profiles of 21 normal samples. We normalized the raw proportional coverage profile using the PoN and segmented the normalized coverage profile. Finally, segmented copy number variants were detected using CallSegments.

Pathway enrichment

We performed pathway enrichment analysis by integrating somatic mutation and CNA data using KOBAS [28] based on the Kyoto Encyclopedia of Genes and Genomes (KEGG) database.

Statistical analysis

The clinicopathological features were analyzed using the SPSS software, version 26.0. Eligible patients were considered as the unmatched cohort. To reduce bias, we also developed a 1:3 (MPMC:PMC) matched cohort using propensity score matching for age, nuclear grade, LVI, TNM stage, and HER2 status with a caliper of 0.10. The variables were compared between groups using Chi-square test. PFS and DDFS curves were drawn using the Kaplan–Meier methods and were compared using log-rank tests. Univariate and multivariate analyses of the patients' survival and the predictors for LNM were performed using the Cox proportional hazards regression model and logistic regression model. The area under the curve of the receiver operating characteristic (ROC) was used to evaluate the discriminative performance of MP% for tumor progression and LNM. ICC was used to estimate the interobserver agreement among four pathologists in MP%. Whole-exome sequencing analyses were conducted using R 3.6.1. The Student's t-test was used to compare significant difference between the two groups in the fraction of genome affected by CNA. The Fisher's exact test was used to compare mutation frequency of genes between groups. All tests were two-sided and a p value <0.05 was considered as statistically significant.

Results

Patient population and clinicopathologic features

In the unmatched cohort, 129 PMCs and 32 MPMCs were found eligible prior to PSM. MPMCs were identified in 19.9% of the breast mucinous carcinomas in this study. The baseline clinicopathological features are summarized in Table 1. All patients were females with a median age of 47 (range, 25–90 years) years. The tumor sizes of breast mucinous carcinomas were mostly between 0.5 and 5.0 cm (T1–T2), with a median size of 2.5 cm. Compared with PMCs, MPMCs occurred at a younger age (median, 42 vs. 46 years; $p = 0.003$) and no significant difference (median, 2.9 vs. 2 cm; $p = 0.356$) in tumor size was observed between them. Morphologically, PMC consisted of neoplastic cells arranged in ribbons, solid sheets, cribriforms, or rarely papillae floating in abundant extracellular mucin. Focal or diffuse micropapillary structures were particularly observed in the MPMC specimens (Fig. 2). Compared with PMCs, MPMCs exhibited higher nuclear grade (low, 3.1 vs. 75.2%; intermediate, 71.9 vs. 24%; high, 25 vs. 0.8%; $p < 0.001$) and histological grade (grade I, 3.1% vs. 68.2%; grade II, 96.9% vs. 31.8%; $p < 0.001$), more frequent LVI (50% vs. 9.3%; $p < 0.001$) and LNM (46.9% vs. 23.2%; $p < 0.001$). The surgical and adjuvant managements of all patients are also shown in Table 1. In contrast to PMCs, more patients with MPMC received adjuvant endocrinotherapy (100 vs. 77.5%; $p = 0.007$) and chemotherapy (59.4 vs. 38.0%; $p = 0.046$).

Biomarkers

The majority of patients with breast mucinous carcinomas were positive for ER (151/161, 93.8%) and PR (137/161, 85.1%) staining. 11 cases were HER2 3+. IHC 2+ staining

Table 1 Characteristics of patients with pure mucinous carcinoma and mucinous carcinoma with micropapillary features.

	Unmatched cohort				Matched cohort[a]			
Variable	All *(N = 161)*	PMC *(N = 129)*	MPMC *(N = 32)*	*p**	All *(N = 28)*	PMC *(N = 21)*	MPMC *(N = 7)*	*p**
Age at diagnosis								
<40	31 (19.3)	20 (15.5)	11 (34.4)	0.003	7 (25.0)	5 (23.8)	2 (28.6)	0.967
40-55	78 (48.4)	60 (46.5)	18 (56.2)		17 (60.7)	13 (61.9)	4 (57.1)	
>55	52 (32.3)	49 (38.0)	3 (9.4)		4 (14.3)	3 (14.3)	1 (14.3)	
Laterality of tumor								
Left	87 (54.0)	73 (56.6)	14 (43.8)	0.269	15 (53.6)	12 (57.1)	3 (42.9)	0.827
Right	74 (46.0)	56 (43.4)	18 (56.2)		13 (46.4)	9 (42.9)	4 (57.1)	
Tumor size (pT)								
pT1	75 (49.3)	67 (51.9)	8 (34.8)	0.112	10 (35.7)	7 (33.3)	3 (42.9)	0.668
pT2	62 (40.8)	51 (39.5)	11 (47.8)		14 (50.0)	11 (52.4)	3 (42.9)	
pT3	6 (3.9)	5 (3.9)	1 (4.3)		2 (7.1)	2 (9.5)	0 (0.0)	
pT4	9 (5.9)	6 (4.7)	3 (13.0)		2 (7.1)	1 (4.8)	1 (14.3)	
Nuclear grade								
low	98 (60.9)	97 (75.2)	1 (3.1)	<0.001	5 (17.9)	4 (19.0)	1 (14.3)	0.776
intermediate	54 (33.5)	31 (24.0)	23 (71.9)		23 (82.1)	17 (81.0)	6 (85.7)	
high	9 (5.6)	1 (0.8)	8 (25.0)		0 (0.0)	0 (0.0)	0 (0.0)	
Histological grade								
Grade I	89 (55.3)	88 (68.2)	1 (3.1)	<0.001	5 (17.9)	4 (19.0)	1 (14.3)	0.776
Grade ii	72 (44.7)	41 (31.8)	31 (96.9)		23 (82.1)	17 (81.0)	6 (85.7)	
Cellularity								
type A (hypocellular)	110 (68.3)	92 (71.3)	18 (56.3)	0.153	17 (60.7)	12 (57.1)	5 (71.4)	0.823
type B (hypercellular)	51 (31.7)	37 (28.7)	14 (43.8)		11 (39.3)	9 (42.9)	2 (28.6)	
LVI								
Positive	32 (19.9)	12 (9.3)	16 (50.0)	<0.001	3 (10.7)	3 (14.3)	0 (0.0)	0.724
Negative	129 (80.1)	117 (90.7)	16 (50.0)		25 (89.3)	18 (85.7)	7 (100.0)	
LNM (pN)								
pN0	129 (80.1)	112 (86.8)	17 (53.1)	<0.001	20 (71.4)	16 (76.2)	4 (57.1)	0.563
pN1	21 (13.1)	13 (10.1)	8 (25.0)		4 (14.3)	2 (9.5)	2 (28.6)	
pN2	7 (4.3)	3 (2.3)	4 (12.5)		3 (10.7)	2 (9.5)	1 (14.3)	
pN3	4 (2.5)	1 (0.8)	3 (9.4)		1 (3.6)	1 (4.8)	0 (0.0)	
TNM staging								
I	74 (46.0)	64 (49.6)	10 (31.3)	0.039	9 (32.1)	6 (28.6)	3 (42.9)	0.717
IIa	48 (29.8)	41 (31.8)	7 (21.9)		8 (28.6)	7 (33.3)	1 (14.3)	
IIb	23 (14.3)	15 (11.6)	8 (25.0)		6 (21.4)	4 (19.0)	2 (28.6)	
IIIa	4 (2.5)	2 (1.6)	2 (6.2)		2 (7.1)	2 (9.5)	0 (0.0)	
IIIb	7 (4.3)	5 (3.8)	2 (6.2)		2 (7.1)	1 (4.8)	1 (14.3)	
IIIc	5 (3.1)	2 (1.6)	3 (9.4)		1 (3.6)	1 (4.8)	0 (0.0)	
ER								
Positive	151 (93.8)	122 (94.6)	29 (90.6)	0.675	23 (82.1)	18 (85.7)	5 (71.4)	0.776
Negative	10 (6.2)	7 (5.4)	3 (9.4)		5 (17.9)	3 (14.3)	2 (28.6)	
PR								
Positive	137 (85.1)	113 (87.6)	24 (75.0)	0.130	23 (82.1)	19 (90.5)	4 (57.1)	0.154
Negative	24 (14.9)	16 (12.4)	8 (25.0)		5 (17.9)	2 (9.5)	3 (42.9)	
HER-2 (OE/GA)								
Amplification	13 (8.1)	4 (3.1)	9 (28.1)	<0.001	2 (7.1)	1 (4.8)	1 (14.3)	0.397
Non-amplification	148 (91.9)	125 (96.9)	23 (71.9)		26 (92.9)	20 (95.2)	6 (85.7)	

Table 1 (continued)

Variable	Unmatched cohort				Matched cohort[a]			
	All *(N = 161)*	PMC *(N = 129)*	MPMC *(N = 32)*	*p**	All *(N = 28)*	PMC *(N = 21)*	MPMC *(N = 7)*	*p**
Ki67								
0–15% +	134 (83.2)	112 (86.8)	22 (68.8)	0.049	25 (89.3)	19 (90.5)	6 (85.7)	0.724
16–50% +	24 (14.9)	15 (11.6)	9 (28.1)		3 (10.7)	2 (9.5)	1 (14.3)	
>50% +	3 (1.9)	2 (1.6)	1 (3.1)		0 (0.0)	0 (0.0)	0 (0.0)	
Local treatment								
Mastectomy	122 (75.8)	102 (79.1)	20 (62.5)	0.003	22 (78.6)	17 (81.0)	5 (71.4)	0.279
Quadrantectomy	13 (8.1)	11 (8.5)	2 (6.3)		2 (7.1)	2 (9.5)	0 (0.0)	
Mastectomy + RT	9 (5.6)	3 (2.3)	6 (18.7)		1 (3.6)	1 (4.8)	0 (0.0)	
Quadrantectomy + RT	17 (10.5)	13 (10.1)	4 (12.5)		3 (10.7)	1 (4.8)	2 (28.6)	
Endocrinotherapy								
Yes	132 (82.0)	100 (77.5)	32 (100)	0.007	18 (64.3)	11 (52.4)	7 (100.0)	0.069
No	29 (18.0)	29 (22.5)	0 (0)		10 (35.7)	10 (47.6)	0 (0.0)	
Chemotherapy								
Yes	68 (42.2)	49 (38.0)	19 (59.4)	0.046	15 (53.6)	11 (52.4)	3 (42.9)	0.827
No	93 (57.8)	80 (62.0)	13 (40.6)		13 (46.4)	10 (47.6)	4 (57.1)	
Radiotherapy								
Yes	26 (16.1)	16 (12.4)	10 (31.3)	0.02	4 (14.3)	2 (9.5)	2 (28.6)	0.279
No	135 (83.9)	113 (87.6)	22 (68.8)		24 (85.7)	19 (90.5)	5 (71.4)	
Local regional recurrence								
Yes	3 (1.8)	0 (0)	3 (9.4)	<0.001	1 (3.6)	0 (0.0)	1 (14.3)	0.078
No	158 (98.1)	129 (100)	29 (90.6)		27 (96.4)	21 (100.0)	6 (85.7)	
Distant metastasis								
Yes	7 (4.3)	4 (3.1)	3 (9.4)	0.283	2 (7.1)	1 (4.8)	1 (14.3)	0.088
No	154 (95.7)	125 (96.9)	29 (90.6)		26 (92.9)	20 (95.2)	6 (85.7)	
Deaths of tumor								
Yes	5 (3.1)	4 (3.1)	1 (3.1)	1.000	0 (0.0)	0 (0.0)	0 (0.0)	-
No	156 (96.9)	125 (96.9)	31 (96.9)		28 (100.0)	21 (100.0)	6 (100.0)	

PMC pure mucinous carcinoma, *MPMC* mucinous carcinoma with micropapillary features, *LVI* peritumoral lymphovascular invasion, *LNM* lymph node metastasis, *ER* estogen recepter, *PR* progesterone receptor, *HER2* human epidermal growth factor receptor 2, *OE* overexpression, *GA* gene amplification, *RT* radiotherapy.

*χ^2 test comparing proportions among PMC group and MPMC group.

[a]Propensity score matching (PSM) was performed using 3:1 nearest neighbor matching with a caliper of 0.10 to accept a matched pair.

was detected in 18 cases, of which 2 cases had amplification of HER2 on FISH. 83.2% (134/161) of the patients had ≤10% positivity for Ki-67. Compared with PMCs, more MPMCs demonstrated HER2 overexpression or gene amplification (28.1 vs. 3.1%; $p < 0.001$) and high Ki67 index (Ki67 > 15% positive, 31.2 vs. 13.2%, $p = 0.049$), while a similar proportion of patients in both groups were positive for ER or PR.

Several studies have demonstrated the utility of reverse polarity or "inside-out" EMA/MUC1 staining in identifying micropapillae, thus all specimens were immunostained with EMA and MUC1 in this cohort (Fig. 2). Diffuse "inside-out" staining pattern of EMA/MUC1 was observed in the micropapillary components within all MPMC cases while most of the PMCs (101/129, 78.2%) exhibited varied cytoplasmic and membrane staining of EMA and MUC1. However, "inside-out" staining pattern was also detected in 28 cases of PMC, of which the tumors were frequently hypocellular with low nuclear grade and were arranged in small clusters.

Interobserver agreement in micropapillary pattern evaluation

Most of the MPMCs (25/32, 78.1%) were characterized by increased cellularity and presented with a MP% of ≥50% (24/32, 75%). The presence of ≥90% of micropapillary features were observed in 10 cases. Rare case of MPMC (1/32, 3.1%) displayed a MP% of <20%. The MP% was then

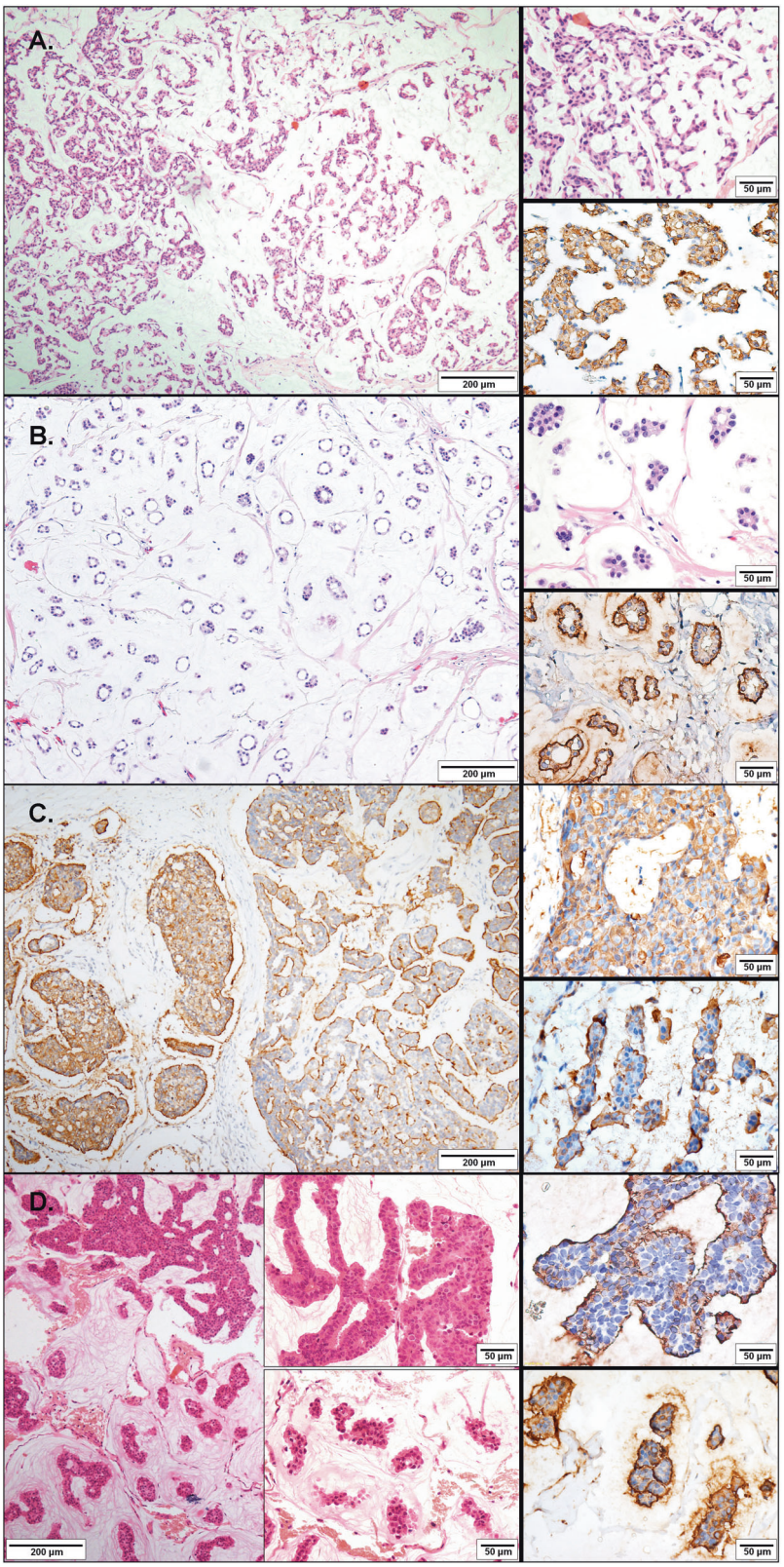

Fig. 2 The morphological and immunohistochemical features of PMC and MPMC. a PMC consisted of neoplastic cells with low nuclear grade arranged in ribbons, floating in abundant extracellular mucin, and demonstrating a cytoplasmic and membrane staining of EMA. **b** Diffuse micropapillary structures were particularly observed in MPMC, with typical "hobnail" cell morphology, showing an "inside-out" EMA immunostaining pattern. **c** The "inside-out" pattern of EMA could also be focally found in PMC. **d** Neoplastic cells arranged in ribbons and focally micropapillaes in MPMC with consistent "inside-out" EMA immunostaining pattern. Original magnification, ×10; inset, ×40.

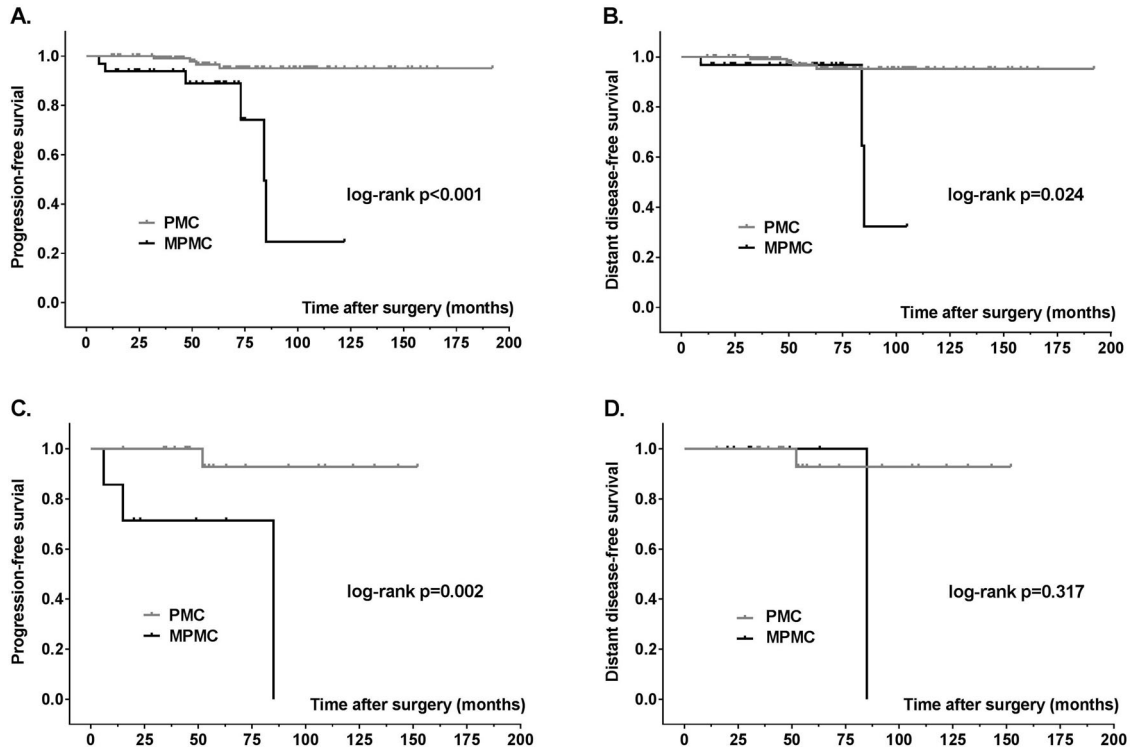

Fig. 3 Survival curves of progression-free survival and distant disease-free survival in MPMC and PMC. Kaplan–Meier curves of PFS (**a**) and DDFS (**b**) between patients with MPMC and PMC in the unmatched cohort. Kaplan–Meier curves of PFS (**c**) and DDFS (**d**) between patients with MPMC and PMC in the matched cohort; using propensity score matching for age, nuclear grade, LVI, TNM stage, and HER2 status.

Table 2 Univariate and multivariate survival analyses for PFS and DDFS.

	Univariable model				Multivariable model			
	p	HR	95% CI lower	95% CI upper	*p*	HR	95% CI lower	95% CI upper
PFS								
pathologic subtypes (PMC vs. MPMC)	<0.001	12.00	3.79	38.03	0.72	1.77	0.08	41.52
MP%	<0.001	1.03	1.01	1.04	0.93	1.00	0.97	1.04
Nuclear grade	0.002	6.36	2.86	14.12	0.03	3.80	1.11	12.97
LVI (negative vs. positive)	0.039	3.19	1.06	9.61	0.48	0.57	0.12	2.67
LNM (negative vs. positive)	0.003	6.31	1.84	21.58	0.09	3.69	0.83	16.35
DDFS								
Pathologic subtypes (PMC vs. MPMC)	0.041	5.03	1.07	23.76	0.34	0.35	0.04	3.07
Nuclear grade	0.001	5.92	2.06	16.99	0.04	6.66	1.09	40.81
LVI (negative vs. positive)	0.005	8.84	1.93	40.55	0.78	1.41	0.13	15.80
LNM (negative vs. positive)	0.021	7.35	1.34	40.29	0.36	2.83	0.31	25.62
HER-2 OE/GA (negative vs. positive)	0.040	4.97	1.07	23.02	0.73	1.50	0.15	14.58
Ki67	0.017	1.06	1.01	1.103	0.73	1.01	0.94	1.09

PMC pure mucinous carcinoma, *MPMC* mucinous carcinoma with micropapillary features; MP%, the percentage of micropapillae, *LVI* lymphovascular invasion, *LNM* lymph node metastasis, *HER2* human epidermal growth factor receptor 2, *OE* overexpression, *GA* gene amplification, *HR* hazard ratio, *CI* confidence interval.

considered in the analyses by predefined categorical groups (<20%, 20–79%, and ≥80%). As shown in Supplementary Fig. 1, the MP% assessment was carried by four different experienced pathologists (PS, JHH, RZL, and ML) and had an excellent interobserver agreement, with an ICC of 0.922 (95% CI 0.901–0.940).

Table 3 Univariate and multivariate analyses for lymph node metastasis.

	Univariable Model				Multivariable Model			
Parameters	*p*	OR	95% CI lower	95% CI upper	*p*	OR	95% CI lower	95% CI upper
Pathologic subtypes (PMC vs. MPMC)	<0.001	5.11	2.13	12.28	0.017	0.01	<0.01	0.48
MP%	<0.001	1.03	1.01	1.04	0.005	1.07	1.02	1.12
LVI (negative vs. positive)	<0.001	18.83	6.96	50.97	<0.001	26.54	7.05	99.90
Tumor size	0.007	1.20	1.05	1.38	0.005	1.20	1.06	1.37
HER2 OE/GA (negative vs. positive)	0.001	4.18	1.75	10.03	0.260	2.25	0.55	9.18
Ki67	0.006	1.05	1.01	1.08	0.234	1.03	0.98	1.08

PMC pure mucinous carcinoma, *MPMC* mucinous carcinoma with micropapillary features; MP%, the percentage of micropapillae, *LVI* lymphovascular invasion, *HER2* human epidermal growth factor receptor 2, *OE* overexpression, *GA* gene amplification, *HR* hazard ratio, CI confidence interval.

Table 4 Recurrence score and potential benefit of chemotherapy for PMCs and MPMCs.

	Recurrence score				Potential extra benefit of chemotherapy[a]		
Pathologic type	≤10 (n/%)	11-25 (n/%)	≥26 (n/%)	*p**	No benefit (n/%)	Benefit (n/%)	*p**
PMC ($n = 12$)	2 (16.7)	5 (41.7)	5 (41.7)	0.185	4 (33.3)	8 (66.7)	0.076
MPMC ($n = 15$)	0 (0.0)	5 (33.3)	10 (66.7)		1 (6.7)	14 (93.3)	

PMC pure mucinous carcinoma, *MPMC* mucinous carcinoma with micropapillary features.

*χ^2 test comparing proportions among PMC group and MPMC group.

[a]According to the results from TAILORx trial, patients at the age of 50 years or younger who had a recurrence score of 0–15 and those over 50 years of age who had a recurrence score ≤25 were classified as no benefit group, otherwise were classified as benefit group.

Prognosis of MPMCs

The patients with PMC were followed-up for 12–192 months, with a median of 67 months. Similarly, MPMCs were followed-up for 14–109 months, with a median of 52 months. Survival analyses were conducted in both unmatched and matched cohorts. The survival curves are shown in Fig. 3. MPMC was associated with a decrease in PFS in both cohorts when comparing to PMC ($p < 0.001$; $p = 0.002$). Patients with MPMC also had a decreased DDFS than patients with PMC in the unmatched cohort ($p = 0.024$) but not in the matched cohort ($p = 0.094$). A Cox proportional hazards regression model was then used to identify the clinicopathological factors affecting the prognosis of patients with PMC. The results are summarized in Table 2. In univariate analyses, MPMC morphology was proved to be a prognostic indicator for PFS (HR = 12.0, 95% CI 3.79–38.03; $p < 0.001$) and DDFS (HR = 5.03, 95% CI 1.07–23.76; $p = 0.041$). However, nuclear grade was the only independent factor for PFS (HR = 3.80, 95% CI 1.11–12.97; $p = 0.03$) and DDFS (HR = 6.66, 95% CI 1.09–40.81; $p = 0.04$) in patients with mucinous carcinoma by multivariate analysis. Moreover, a logistic regression model was also applied to estimate the clinicopathological factors affecting the incidence of LNM (Table 3). The MP%, LVI, and tumor size were identified as significant and independent factors for LNM in univariate and multivariate analyses. The optimal cut-off value of MP% determined by the ROC curve was 17.5% for both tumor progression (AUC = 0.705; sensitivity 56.3%; specificity 84.8%) and LNM (AUC = 0.663; sensitivity 42.4%; specificity 88.2%) in patients with mucinous carcinoma (Supplementary Fig. 2).

Recurrence score of PMCs

The recurrence scores of the selected PMCs and MPMCs are summarized in Table 4. Only 2 (7.4%) patients with PMC had a recurrence score of 0–10 (low risk). The recurrence score in MPMCs was higher than in PMCs (median, 30.58 vs. 19.32), but no statistical difference was observed between groups ($p = 0.185$). Moreover, we also observed that more patients with MPMC (14/15, 93.3%) might likely to benefit from additional chemotherapy than patients with PMC (8/12, 66.7%) according to the recommendation by TAILORx trial [22], however, no statistical difference was found between groups ($p = 0.076$).

Profiles of somatic mutations in breast mucinous carcinomas

Paired FFPE tissues and adjacent normal tissues from 21 breast mucious carcinomas, including 10 MPMCs and 11

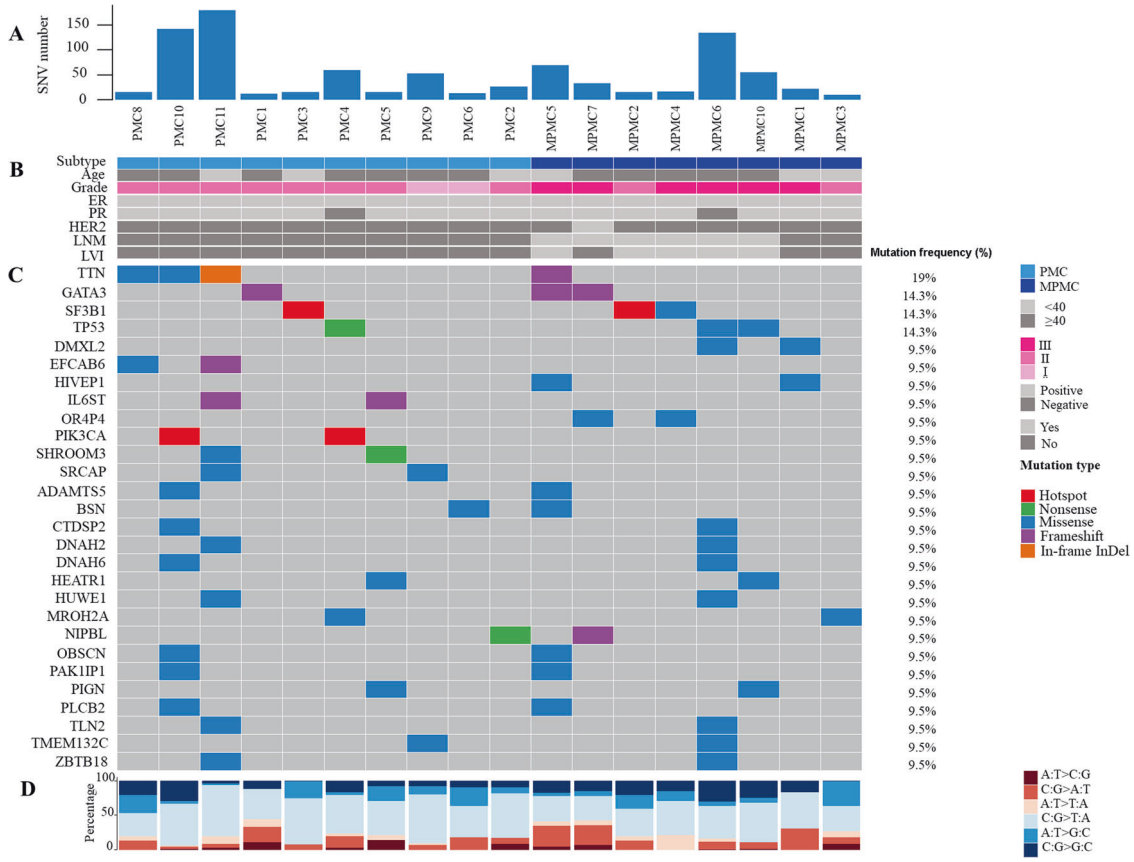

Fig. 4 Somatic mutational landscape of MPMC and PMC. Twenty-one patients with breast mucinous carcinoma are arranged along the *x*-axis (10 MPMCs and 11 PMCs). MPMC9, MPMC12 and PMC7 harboring no overlapping mutated genes with other samples were not displayed. **a** Number of single nucleotide variants is shown with each column representing one particular case. **b** Clinicopathological characteristics are depicted via the phenotype bars. **c** Representation of the recurrent somatic mutations across this cohort. The mutation frequency of each gene in PMC is listed on the right side. **d** The mutation spectrum of each sample.

PMCs were eligibled and collected for WES. Clinicopathological features of the selected patients are listed in Supplementary Table 1. WES data were analyzed with a mean coverage of 124.9× (range, 76.3–206.2×). The sequenced reads covered 92.6% of bases of genomic region by 30× (range, 76.8–96.3%) (Supplementary Table 2). First, the genomic landscape of breast mucinous carcinomas is shown in Fig. 4. 938 somatic mutations including 782 missenses, 81 frameshifts, 49 nonsenses, and 26 in-frame InDels were identified in breast mucinous carcinomas (Supplementary Table 3). TTN (19.1%, 4/21), GATA3 (14.3%, 3/21), SF3B1 (14.3%, 3/21), and TP53 (14.3%, 3/21) were the most frequently mutated genes. Notably, PMCs tended to display a relative low frequency of TP53 (14.3%) and PIK3CA (9.5%) mutations. Moreover, we observed a relative high frequency of SF3B1 mutations (14.3%), of whom two cases displayed SF3B1 K700E hotspot mutation. Point substitutions were classified into six mutational profiles according to the direction of mutation, and the predominant mutational profile was C:G > T:A. The median somatic mutation rate was 0.27 (range, 0.1–3.0) per Mb, indicating a low mutation rate. Potential association between the somatic mutations number with age, grade, and tumor size were examined using a generalized linear model. No significant relationship was observed between any clinical feature and mutation number.

Mutational repertoire in MPMCs and PMCs

MPMCs may be morphologically and clinically distinct from PMCs, and whether they harbored specific genomic alterations has yet to be characterized. A total of 552 somatic mutations were identified in PMCs including 451 missenses, 58 frameshifts, 25 nonsenses, and 18 In-frame InDels, while 386 somatic mutations were found in MPMCs including 331 missenses, 23 frameshifts, 24 nonsenses, and 8 In-frame InDels. The overall landscape of mutations per case is depicted in Fig. 4. TTN (27.3%), PIK3CA (18.2%) mutations were frequently found in PMCs, while GATA3 (20%), TP53 (20%) and SF3B1

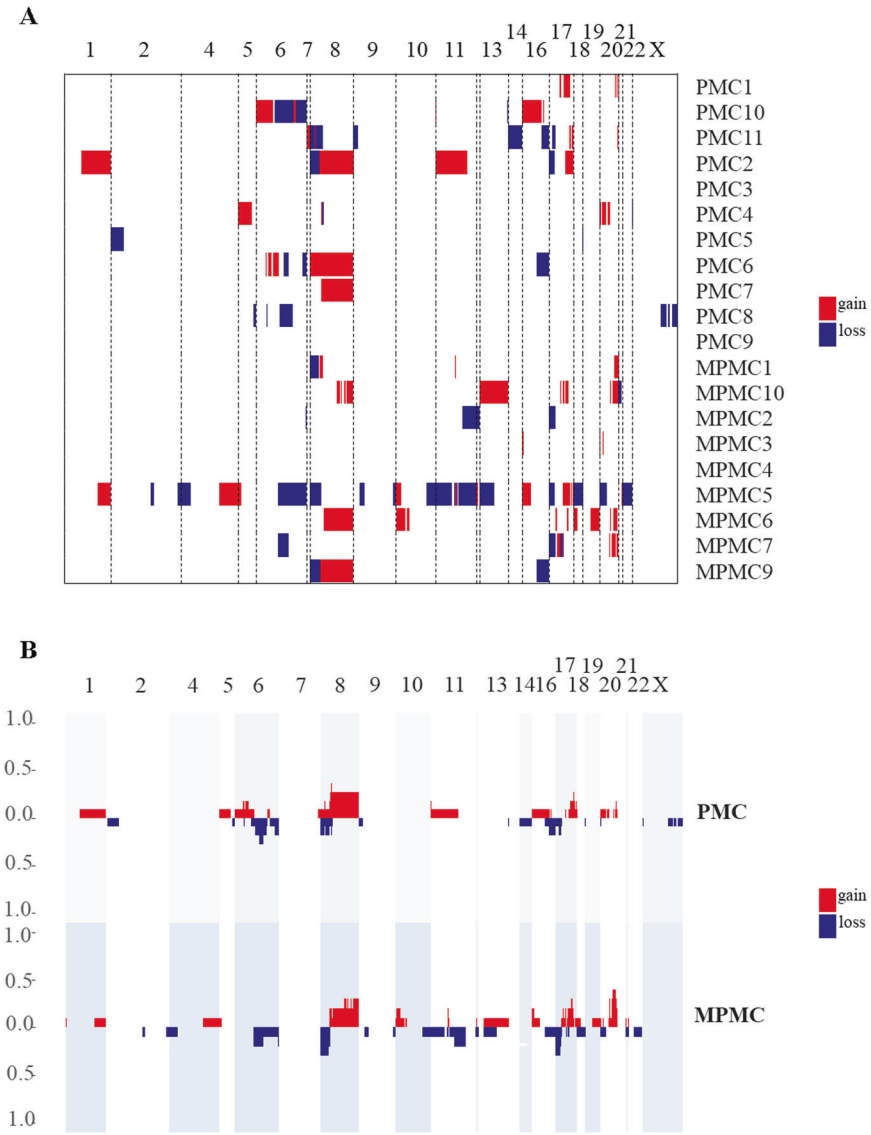

Fig. 5 Copy number aberrations identified in MPMCs and PMCs. a Copy number gains (red) or losses (blue) for each case are displayed. Cases are listed in rows and chromosomes along the *x*-axis. **b** Frequency plots depicted the frequency of gains (blue bar) or losses (red bar) for each gene according to genomic positions.

(20%) were recurrently mutated in MPMCs. PIK3CA hotspot mutations (E545K and M1043I) were exclusively detected in PMCs. Only one case (PMC8) harbored HER2 mutation (p.V1184L), which was not in the extracellular domain of HER2 and not reported in COMSIC. Notably, only 20 genes carried at least one mutation site were shared by MPMCs and PMCs. These results may indicate that MPMC was also genetically distinct from PMC.

Somatic copy number aberrations in MPMCs and PMCs

As shown in Fig. 5, MPMCs and PMCs harbored few CNAs. MPMCs harbored significant arm-level alteration including chromosomal gains at 8q, 17q, and 20q, as well as chromosomal losses at 6q, 17p. Meanwhile, significant gains at 6p, 8q, as well as deleted regions at 6q, were examined in PMCs. Recurrent 6q14.1-q27 losses and 8p11.21-q24.3 gains tended to be shared by MPMCs and PMCs, indicating that these CNAs were prevalent in breast mucinous carcinoma. When the arm-level CNV was compared with ER + /HER2- breast cancer, none of the MPMC and PMC were found to harbor 1q whole-arm gains and 16q whole-arm losses. Copy number gain of the HER2 was exclusively found in two MPMCs (2/10). Consistent with the HER2 positive status by IHC and FISH, copy gain of HER2 was observed in MPMC7. Interestingly, HER2 gain was also detected in MPMC10, which was negative by IHC or FISH, revealing the existence of tumor heterogeneity. Specifically, a loss of the tumor suppressor gene TP53 on 17p displayed a higher prevalence in MPMC (3/10) than in PMC (1/11). Besides, the fraction of genome altered by copy number alteration showed no significant difference between MPMCs and PMCs.

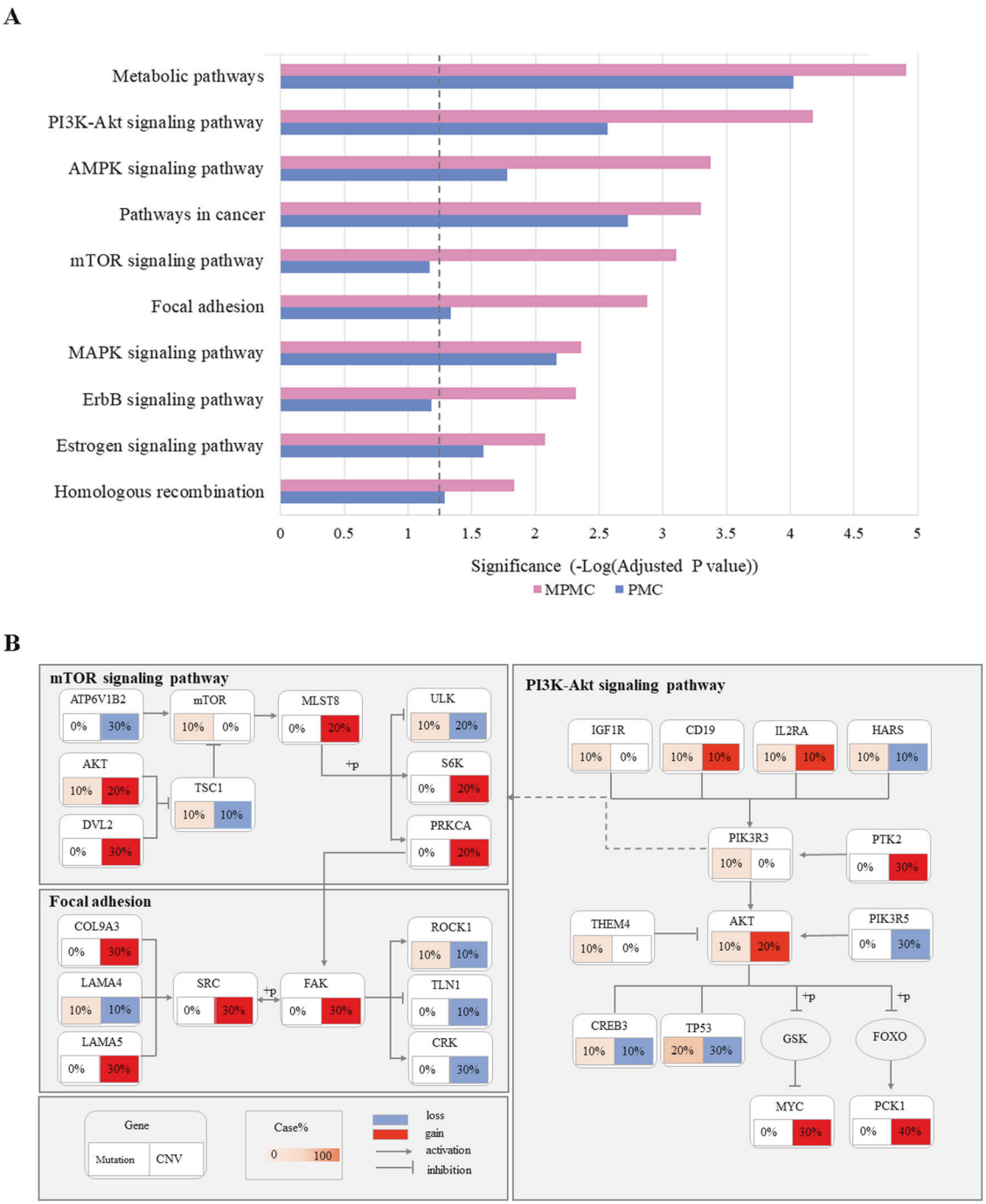

Fig. 6 Altered signaling pathways in MPMCs. a Representative KEGG signaling pathways were altered more significantly in MPMCs than in PMCs. The significance level [-log10(p value)] is also shown for each gene as bar charts. **b** Alterations including mutations, copy number gains, and losses affecting the PIK3-Akt/mTOR/focal adhesion signaling pathways.

Altered signaling pathways in MPMCs

Several KEGG signaling pathways were more significantly mutated in MPMCs compared with PMCs (Fig. 6a). Notably, the mTOR (adjusted $p = 0.003$) and ErbB signaling pathways (adjusted $p = 0.004$) were significantly altered in MPMCs, which were not significantly in PMCs (Supplementary Table 4). The mutation of PIK3R3, mTOR, and HRAS affected both the PI3K-Akt, mTOR, and ErbB pathways. Copy number gains of Myc and HER2 dysregulated the ErbB pathway. In addition, the activation of CD19 and IL2RA (mutations and gains), and the inactivation of TP53, HRAS and CREB3 (mutations and losses) predominately resulted in the deregulation of the PI3K-Akt pathway (Fig. 6b). We also

identified alterations frequently affecting the mTOR pathway, including mutations in ATP6V1B1, TSC2, and ULK2. Besides, focal adhesion that plays essential roles in important biological processes including cell motility and cell proliferation was also more significantly mutated in MPMCs (Fig. 6a). Copy number gains frequently occurred in SRC (30%), LAMA5 (30%), and COL9A3(30%), which would over-activate the focal adhesion kinase, resulting in invasion and metastasis (Fig. 6a). Interestingly, one of the patients with MPMC (MPMC-6), who relapsed within three months after surgery had significant enrichment in both the PI3K-Akt ($p = 0.008$), mTOR ($p = 0.010$) and focal adhesion ($p = 0.010$) pathways.

Discussion

Mucinous carcinoma of the breast is an uncommon subtype of invasive breast carcinoma characterized by clusters of epithelial tumor cells suspended in pools of extracellular mucin. Pure mucinous carcinoma, requiring a mucinous component of over 90%, is generally associated with low recurrence rate and favorable 5-20 years survival [3]. However, local recurrence or late distant metastasis is found in a minority. It is clinically important to identify the patients with PMC that in risk of worse prognosis, and to develop an appropriate treatment for them. Siriaunkgul, et al. [29] first described micropapillary structure in breast carcinoma and confirmed it as a special type of breast carcinoma named "invasive micropapillary carcinoma," which is associated with a more aggressive biological behavior, such as frequent LVI and LNM. Subsequently, the micropapillary features were also recognized in mucinous carcinoma since the first report by Ng [30] in 2002 and the term "mucinous carcinoma with micropapillary features" has been used as reference to 2019 WHO classification of breast tumors (5th edition) [19]. However, whether MPMC can be identified as a morphologically, clinically or genetically distinct entity from PMC remains controversial.

The present study showed that ~19.9% of breast mucinous carcinomas were classified as MPMC. Previous studies suggested the incidence of MPMC in breast mucinous carcinomas was 14.9–47.2%, which may predominantly due to the lack of a defined diagnostic criteria. Morphologically, tumor arranged in small solid clusters, rings or tubules with crisp or serrated peripheral borders, lack of fibrovascular core, typical "hobnail" cell morphology, frequent psammomatous calcifications, and adjacent micropapillary DCIS were commonly used as supporting evidence for the diagnosis. Besides, Shet et al. [16] and Xu et al. [14] defined MPMC as mucinous carcinoma with diffuse micropapillary features or a MP% of >90%, while studies by Liu et al. [10] and Kim et al. [12] included patients with a MP% of >50%. The cut-off value of MP% for the diagnosis of MPMC was not mentioned in several studies [17, 18]. Despite that we used a loose criteria in this study in which mucinous carcinoma containing any percentage of micropapillaes (MP% ≥1%) and with any nuclear grade was classified as MPMC. MPMCs included in the present study displayed a MP% ranging from 5 to 100%, of which 75% presented with a MP% of ≥50%. Furthermore, the MP% assessment was carried by four experienced pathologists and their assessment had an excellent inter-observer agreement, while the "inside-out" EMA/MUC1 immunostaining pattern, which had been considered as a confirmatory method in identifying micropapillae, was also observed in 21.7% of PMCs consisting with previous studies [10, 18]. Thus, the identification of micropapillae should be based on morphologic criteria and reversed polarity MUC1/EMA staining which may serve as a supplement until specific diagnostic tests become available.

Next, we investigated whether the presence of micropapillary features affected the clinical biological behavior of breast mucinous carcinomas. PMC is considered traditionally as a less aggressive breast carcinoma with low to moderate nuclear grade, low HER2 expression, rare LVI, and LNM. Most studies have demonstrated that MPMC exhibited more frequent LVI (14.2–60%) and LNM (9.1–53.3%) than PMC. In one retrospective series by Liu et al. [10], MPMC patients had a significantly decreased overall survival and recurrence-free survival than PMC, and the micropapillary feature was confirmed as an independent unfavorable predictor for recurrence-free survival in mucinous carcinoma. However, conflicting results have been reported. Bal et al. [11] described six cases of MPMC with the low nuclear grade, and no LNM was observed. In a study by Xu et al. [14], 60 breast mucinous carcinomas with a diffuse or focal micropapillary structure of low to intermediate nuclear grade and no local recurrence or distant metastasis was observed. They suggested that the clinicopathological features of MPMC, such as high nuclear grade, HER2 amplification, may predominantly contribute to their clinical behavior rather than micropapillary architecture itself. According to our data, compared with PMC, MPMC occurred in younger age patients and exhibited higher nuclear grade, higher incidence of HER2 overexpression or gene amplification, and more frequent LVI and LNM. MPMC was also associated with decreased PFS and DDFS when compared with PMC. Although MPMC was an independent factor for either PFS or DDFS in multivariate analysis, MPMCs were still associated with a numerically inferior PFS than PMCs after matching for age, nuclear grade, LVI, TNM stage, and HER2 status. These results indicated that MPMC could be considered as an aggressive subtype of mucinous carcinoma distinct from PMC. Notably, multivariate analyses confirmed MP% as an independent unfavorable predictor for LNM, while nuclear grade was identified

as the only independent unfavorable factor for PFS and DDFS.

Our findings highly suggest that pathologists should also evaluate nuclear grade and MP% prior to making a diagnosis of MPMC, which may identify those in risk of worse prognosis. Considering the higher risks of LVI and LNM in MPMCs, some investigators suggested that sentinel lymph node biopsy and/or axillary lymph node dissection should be more actively performed in MPMCs, followed by more aggressive postoperative therapy [10]. Our study also showed that more patients with MPMC received adjuvant endocrinotherapy and chemotherapy than PMCs. However, the results may have been influenced by the higher rate of T and N stage of tumors in the MPMC group than in the PMC group, and no significant difference was observed in surgery or adjuvant therapy between the groups in the matched cohort. A recurrence score by the 21-gene assay is believed to be able to predict the benefit from adjuvant chemotherapy in ER+ disease [22]. Most PMC had a low or intermediate RS, and few cases had a RS of >25 [31, 32]. Despite 66.7% of MPMCs were in high risk with a RS of >25 in our cohort, and more MPMCs might likely to benefit from additional chemotherapy than PMCs using the recommendations by TAILORx trial integrating age factor [22], however, given the small sample size, no statistical difference was observed between MPMCs and PMCs. Our findings suggested that even if MPMC is clinically distinct from PMC, there is currently no sufficient evidence supporting that the patients with MPMC should receive relatively more aggressive treatments.

A recent study portrayed the genomic landscape of breast mucinous carcinoma, which represents a genetically distinct form of ER + /HER2− breast cancer [33]. Similarly, our data also showed that PMCs had a low mutational burden, harbored less mutations affecting TP53, PIK3CA, and exhibited no concurrent 1q gains and 16q losses, which are prevalent in ER-positive breast cancer [34]. Besides, we also conducted a comparative analysis to address whether MPMC exhibited genetic features distinct from PMC, and whether these specific genomic alterations were responsible for the aggressive tumor behavior of MPMC. We found that MPMCs shared some genetic alterations with PMCs, such as low somatic mutation burden, common mutations affecting TTN, GATA3, SF3B1, TP53, recurrent 6q14.1-q27 losses, and 8p11.21-q24.3 gains. However, MPMCs still harbored specific genomic alterations distinct from PMCs such as GATA3, TP53, and SF3B1 which were recurrently mutated in MPMCs while PIK3CA mutations were exclusively detected in PMCs. Moreover, MPMCs harbored 17q and 20q gains as well as 17p losses, while PMCs displayed gains at 6p. Pareja et al. [15] hypothesized that some MPMCs may be stemmed from invasive micropapillary carcinomas (IMPC) and bore similarities in genomic features with them, including recurrent gains at the 8q, 17q, and 20q as reported in a previous study [35]. Nevertheless, specific somatic mutations affecting the mitogen-activated protein kinase family (MAP3K1, MAP2K6, and MAP3K4), NBPF10, PIK3CA, which were described in IMPC [35] were not observed in any of the MPMCs according to our data. Genomic drivers may vary dramatically in different cancers with micropapillary architecture. For example, mutations in the extracellular domain of ERBB2, including S310F, S310Y, and R157W were identified in 40% of micropapillary urothelial carcinoma [36]. EGFR mutation was present in 65–76% of lung adenocarcinoma with micropapillary pattern [37, 38].

Given that MPMC displayed a more aggressive behavior, the underlying mechanism of oncogenicity is of special interest. Combined with somatic mutation analysis and copy number aberration (CNA) analysis, our result indicated that several oncogenic pathways were more frequently deregulated in MPMC than in PMC, including the PI3K-Akt, mTOR, AMPK, ErbB, and focal adhesion signaling pathways. The PI3K/Akt/mTOR pathways were frequently associated with aggressive metastasis and invasiveness in various cancers [39–43]. Several core elements altered in these pathways are depicted (Fig. 6). Notably, the mTOR pathway was frequently altered by AKT2, AKT3, including somatic mutations and copy number gains (20%). AKT phosphorylates several substrates, leading to the overactivity of mTOR. On one hand, mTOR phosphorylates ULK1, thereby preventing its activation by AMPK resulting in defective autophagy [44–48]. On the other hand, S6K1, the substrate of mTOR, overactivates a critical component of ribosome synthetase and facilitates protein synthesis, cell proliferation, and growth [49–51]. Interestingly, we found that focal adhesion pathway, which plays essential roles in important biological processes including cell proliferation, cancer cell migration, invasion, and metastasis [52–54], was also more significantly dysregulated in MPMC. In our study, the copy number gains of SRC, FAK, and PRKCA accounted for the core elements of the focal adhesion pathway. Accumulating evidence suggests that the FAK/SRC complex could promote the activation of Rac1and JNK and results in matrix metalloproteinase-mediated extracellular matrices proteolysis, which is pivotal for cancer cell invasion through changes in focal adhesion and cytoskeletal dynamics [55–57]. Besides, the overexpression and activation of FAK/SRC are often associated with breast cancer invasion [58, 59]. Therefore, the focal adhesion pathway could be considered as a potential therapeutic target. These results have provided evidence that MPMC could be genetically distinct from PMC and the specific genomic alterations observed in MPMC may be responsible for the aggressive tumor behavior.

One limitation of the present study was the small number of cases included in the genomic analysis. Inclusion of a larger cohort could be crucial and offer more practical

insights. Besides, previous study [10, 16] suggests that MPMC may be an entity under the morphologic spectrum of IMPC. However, our cohort does not include patients with IMPC and we only preliminarily compared the differences of genetic profiles between MPMC and IMPC of breast referring to the literature [35]. Further integrated multi-omics analyses are necessary to fully unveil the genomic architecture and tumor spectrums among MPMC, PMC, and IMPC. Nonetheless, findings from our study delineated a comprehensive view of breast mucious carcinomas and revealed that MPMC is morphologically, clinically, and genetically distinct from PMC. The specific genomic alterations carried by MPMCs may be responsible for the aggressive tumor behavior.

Data availability

The datasets generated and/or analysed during the current study are also available from the corresponding author on reasonable request.

Funding This study was funded by the Guangdong Medical Research Foundation (A2018241) and National Natural Science Foundation of China (81902679) in the design of the study and collection, analysis, and interpretation of data and in writing the manuscript.

Author contributions Conceptualisation: PS, JH; Data acquisition: PS, ZZ, QL, XC, DC, HW; Methodology: PS, ZZ, QL, ML, JH; Data analysis: PS, ML, RL, JH, ZZ, DC, HW; Writing original draft and editing: PS, ZZ, JH; Data curation: PS, JH; Project administration: PS, JH; Funding acquisition: PS. All authors read and approved the final manuscript.

Compliance with ethical standards

Ethics approval and consent to participate All procedures performed in studies involving human participants were in accordance with the ethical standards of the Sun Yat-sen University Cancer Center (SYSUCC) research committee and with the 1964 Helsinki declaration and its later amendments or comparable ethical standards. The formal written informed consent was obtained from all individual participants included in the study.

Conflict of interest The authors declare that they have no conflict of interest.

References

1. Diab SG, Clark GM, Osborne CK, Libby A, Allred DC, Elledge RM. Tumor characteristics and clinical outcome of tubular and mucinous breast carcinomas. J Clin Oncol. 1999;17:1442–8.
2. Yerushalmi R, Gelmon KA, Barkley CR, Ligibel JA, Wong JS. Mucinous breast carcinoma: a large contemporary series. Am J Surg. 2018;196:549–51.
3. Di Saverio S, Gutierrez J, Avisar EA. Retrospective review with long term follow up of 11,400 cases of pure mucinous breast carcinoma. Breast Cancer Res Treat. 2008;111:541–7.
4. Wang J, Tang H, Li X, Song C, Xiong Z, et al. Is surgical axillary staging necessary in women with T1 breast cancer who are treated with breast-conserving therapy? Cancer Commun. 2019;39:25.
5. Makki J. Diversity of breast carcinoma: histological subtypes and clinical relevance. Clin Med Insights Pathol. 2015;8:23–31.
6. Skotnicki P, Sas-Korczynska B, Strzepek L, Jakubowicz J, Blecharz P, Reinfuss M, et al. Pure and mixed mucinous carcinoma of the breast: a comparison of clinical outcomes and treatment results. Breast J. 2016;22:529–34.
7. Dumitru A, Procop A, Iliesiu A, Tampa M, Cirstoiu M. Mucinous breast cancer: a review study of 5 year experience from a hospital-based series of cases. Maedica. 2015;10:14–8.
8. Ranade A, Batra R, Sandhu G, Chitale RA, Balderacchi J. Clinicopathological evaluation of 100 cases of mucinous carcinoma of breast with emphasis on axillary staging and special reference to a micropapillary pattern. J Clin Pathol. 2010;63:1043–7.
9. Yang YL, Liu BB, Zhang X, Fu L. Invasive micropapillary carcinoma of the breast: an update. Arch Pathol Lab Med. 2016;140:799–805.
10. Liu F, Yang M, Li Z, Guo X, Lin Y, Lang R, et al. Invasive micropapillary mucinous carcinoma of the breast is associated with poor prognosis. Breast Cancer Res Treat. 2015;151:443–51.
11. Bal A, Joshi K, Sharma SC, Das A, Verma A, Wig JD. Prognostic significance of micropapillary pattern in pure mucinous carcinoma of the breast. Int J Surg Pathol. 2008;16:251–6.
12. Kim HJ, Park K, Kim JY, Kang G, Gwak G, Park I. Prognostic significance of a micropapillary pattern in pure mucinous carcinoma of the breast: comparative analysis with micropapillary carcinoma. J Pathol Transl Med. 2017;51:403–9.
13. Collins K, Ricci AJ. Micropapillary variant of mucinous breast carcinoma: a distinct subtype. Breast J. 2018;24:339–42.
14. Xu X, Bi R, Shui R, Yu B, Cheng Y, Tu X, et al. Micropapillary pattern in pure mucinous carcinoma of the breast–does it matter or not? Histopathology. 2019;74:248–55.
15. Pareja F, Selenica P, Brown DN, Sebastiao APM, da Silva EM, Da Cruz Paula A, et al. Micropapillary variant of mucinous carcinoma of the breast shows genetic alterations intermediate between those of mucinous carcinoma and micropapillary carcinoma. Histopathology. 2019;75:139–45.
16. Shet T, Chinoy R. Presence of a micropapillary pattern in mucinous carcinomas of the breast and its impact on the clinical behavior. Breast J. 2008;14:412–20.
17. Barbashina V, Corben AD, Akram M, Vallejo C, Tan LK. Mucinous micropapillary carcinoma of the breast: an aggressive counterpart to conventional pure mucinous tumors. Hum Pathol. 2013;44:1577–85.
18. Troxell ML. Reversed MUC1/EMA polarity in both mucinous and micropapillary breast carcinoma. Hum Pathol. 2014;45:432–4.
19. WHO Classificaion of Tumours Editorial Board. Breast tumours. Lyon (France): International Agency for Research on Cancer; (WHO Classification of tumours series, 5th ed.; vol. 2) 2019.
20. Hammond ME, Hayes DF, Dowsett M, Allred DC, Hagerty KL, et al. American Society of Clinical Oncology/College Of American Pathologists guideline recommendations for immunohistochemical testing of estrogen and progesterone receptors in breast cancer. J Clin Oncol. 2010;28:2784–95.
21. Wolff AC, Hammond MEH, Allison KH, Harvey BE, Mangu PB, et al. Human epidermal growth factor receptor 2 testing in breast cancer: American society of clinical oncology/college of american pathologists clinical practice guideline focused update. J Clin Oncol. 2018;36:2105–22.

22. Sparano JA, Gray RJ, Makower DF, Pritchard KI, Albain KS, Hayes DF, et al. Adjuvant chemotherapy guided by a 21-gene expression assay in breast cancer. N. Engl J Med. 2018;379:111–21.
23. Van der Auwera GA, Carneiro MO, Hartl C, Poplin R, Del Angel G, Levy-Moonshine A, et al. From FastQ data to high confidence variant calls: the genome analysis toolkit best practices pipeline. Curr Protoc Bioinforma. 2013;43:11.10.1–33.
24. Li H. Exploring single-sample SNP and INDEL calling with whole-genome de novo assembly. Bioinformatics. 2012;28:1838–44.
25. Sherry ST, Ward MH, Kholodov M, Baker J, Phan L, Smigielski EM, et al. dbSNP: the NCBI database of genetic variation. Nucleic Acids Res. 2001;29:308–11.
26. 1000 Genomes Project Consortium, Abecasis GR, Auton A, Brooks LD, DePristo MA, Durbin RM, et al. An integrated map of genetic variation from 1,092 human genomes. Nature. 2012;491:56–65.
27. Wang K, Li M, Hakonarson H. ANNOVAR: functional annotation of genetic variants from high-throughput sequencing data. Nucleic Acids Res. 2010;38:e164.
28. Xie C, Mao X, Huang J, Ding Y, Wu J, Dong S, et al. KOBAS 2.0: a web server for annotation and identification of enriched pathways and diseases. Nucleic Acids Res. 2011;39:W316–22.
29. Siriaunkgul S, Tavassoli FA. Invasive micropapillary carcinoma of the breast. Mod Pathol. 1993;6:660–2.
30. Ng WK. Fine-needle aspiration cytology findings of an uncommon micropapillary variant of pure mucinous carcinoma of the breast: review of patients over an 8-year period. Cancer 2002;96:280–8.
31. Wu J, Ding S, Lin L, Fei X, Lin C, Andriani L, et al. Comparison of the distribution pattern of 21-gene recurrence score between mucinous breast cancer and infiltrating ductal carcinoma in chinese population: a retrospective single-center study. Cancer Res Treat. 2020;10:4143.
32. Turashvili G, Brogi E, Morrow M, Hudis C, Dickler M, Norton L, et al. The 21-gene recurrence score in special histologic subtypes of breast cancer with favorable prognosis. Breast Cancer Res Treat. 2017;165:65–76.
33. Pareja F, Lee JY, Brown DN, Piscuoglio S, Gularte-Mérida R, Selenica P, et al. The genomic landscape of mucinous breast cancer. J Natl Cancer Inst. 2019;111:737–41.
34. Lacroix-Triki M, Suarez PH, MacKay A, Lambros MB, Natrajan R, Savage K, et al. Mucinous carcinoma of the breast is genomically distinct from invasive ductal carcinomas of no special type. J Pathol. 2010;222:282–98.
35. Natrajan R, Wilkerson PM, Marchiò C, Piscuoglio S, KY Ng C, Wai P, et al. Characterization of the genomic features and expressed fusion genes in micropapillary carcinomas of the breast. J Pathol. 2014;232:553–65.
36. Ross JS, Wang K, Gay LM, Al-Rohil RM, Nazeeret T, et al. A high frequency of activating extracellular domain ERBB2 (HER2) mutation in micropapillary urothelial carcinoma. Clin Cancer Res. 2014;20:68–75.
37. Borczuk AC. Micropapillary histology: a frequent morphology of mutation-associated lung adenocarcinoma? Am J Clin Pathol. 2009;131:615–7.
38. Zhang J, Sun J, Zhang Z, Wang A, Liang X, et al. Driver mutation profiles and clinicopathological correlation in pulmonary adenocarcinoma with a micropapillary component. Hum Pathol. 2019;85:242–50.
39. Chen M, Gu J, Delclos GL, Killary AM, Fan Z, Hildebrandt MA, et al. Genetic variations of the PI3K-AKT-mTOR pathway and clinical outcome in muscle invasive and metastatic bladder cancer patients. Carcinogenesis. 2010;31:1387–91.
40. Luo C, Cen S, Ding G, Wu W. Mucinous colorectal adenocarcinoma: clinical pathology and treatment options. Cancer Commun (Lond). 2019;39:13.
41. Pierobon M, Ramos C, Wong S, Hodge KA, Aldrich J, Byron S, et al. Enrichment of PI3K-AKT-mTOR pathway activation in hepatic metastases from breast cancer. Clin Cancer Res. 2017;23:4919–28.
42. Scartozzi M, Giampieri R, Maccaroni E, Mandolesi A, Biagetti S, Alfonsi S, et al. Phosphorylated AKT and MAPK expression in primary tumours and in corresponding metastases and clinical outcome in colorectal cancer patients receiving irinotecan-cetuximab. J Transl Med. 2012;10:71.
43. Bai H, Li H, Li W, Gui T, Yang J, Cao D, et al. The PI3K/AKT/mTOR pathway is a potential predictor of distinct invasive and migratory capacities in human ovarian cancer cell lines. Oncotarget. 2015;6:25520–32.
44. Egan D, Kim J, Shaw RJ, Guan KL. The autophagy initiating kinase ULK1 is regulated via opposing phosphorylation by AMPK and mTOR. Autophagy. 2011;7:643–4.
45. Nazio F, Strappazzon F, Antonioli M, Bielli P, Cianfanelli V, Bordi M, et al. mTOR inhibits autophagy by controlling ULK1 ubiquitylation, self-association and function through AMBRA1 and TRAF6. Nat Cell Biol. 2013;15:406–16.
46. Petherick KJ, Conway OJ, Mpamhanga C, Osborne SA, Kamal A, Saxty B, et al. Pharmacological inhibition of ULK1 kinase blocks mammalian target of rapamycin (mTOR)-dependent autophagy. J Biol Chem. 2015;290:28726.
47. Suvorova II, Pospelov VA. AMPK/Ulk1-dependent autophagy as a key mTOR regulator in the context of cell pluripotency. Cell Death Dis. 2019;10:260.
48. Kim J, Kundu M, Viollet B, Guan KL. AMPK and mTOR regulate autophagy through direct phosphorylation of Ulk1. Nat Cell Biol. 2011;13:132–41.
49. Ben-Sahra I, Howell JJ, Asara JM, Manning BD. Stimulation of de novo pyrimidine synthesis by growth signaling through mTOR and S6K1. Science. 2013;339:1323–8.
50. Yamnik RL, Digilova A, Davis DC, Brodt ZN, Murphy CJ, Holz MK. S6 kinase 1 regulates estrogen receptor alpha in control of breast cancer cell proliferation. J Biol Chem. 2009;284:6361–9.
51. Khotskaya YB, Goverdhan A, Shen J, Ponz-Sarvise M, Chang SS, Hsu MC, et al. S6K1 promotes invasiveness of breast cancer cells in a model of metastasis of triple-negative breast cancer. Am J Transl Res. 2014;6:361–76.
52. Yom CK, Noh DY, Kim WH, Kim HS. Clinical significance of high focal adhesion kinase gene copy number and overexpression in invasive breast cancer. Breast Cancer Res Treat. 2011;128:647–55.
53. Bijian K, Lougheed C, Su J, Xu B, Yu H, Wu JH, et al. Targeting focal adhesion turnover in invasive breast cancer cells by the purine derivative reversine. Br J Cancer. 2013;109:2810–8.
54. Mirza AA, Kahle MP, Ameka M, Campbell EM, Cuevas BD. MEKK2 regulates focal adhesion stability and motility in invasive breast cancer cells. Biochim Biophys Acta. 2014;1843:945–54.
55. Sulzmaier FJ, Jean C, Schlaepfer DD. FAK in cancer: mechanistic findings and clinical applications. Nat Rev Cancer. 2014;14:598–610.
56. McLean GW, Carragher NO, Avizienyte E, Evans J, Brunton VG, Frame MC. The role of focal-adhesion kinase in cancer - a new therapeutic opportunity. Nat Rev Cancer. 2015;5:505–15.
57. Luo M, Guan JL. Focal adhesion kinase: a prominent determinant in breast cancer initiation, progression and metastasis. Cancer Lett. 2010;289:127–39.
58. Annis MG, Ouellet V, Rennhack JP, L'Esperance S, Rancourt C, Mes-Masson A, et al. Integrin-uPAR signaling leads to FRA-1 phosphorylation and enhanced breast cancer invasion. Breast Cancer Res. 2018;20:9.
59. Chan KT, Cortesio CL, Huttenlocher A. FAK alters invadopodia and focal adhesion composition and dynamics to regulate breast cancer invasion. J Cell Biol. 2009;185:357–70.